PERGAMON

Mechatronics 11 (2001) 59–77

MECHATRONICS

Optimal construction and control of flexible manipulators: a case study based on LQR output feedback

Pixuan Zhou[a,b], Fei-Yue Wang[a,b,*], Weinong Chen[c], Paul Lever[d]

[a]*The Intelligent Control and Systems Engineering Center, Chinese Academy of Sciences, Beijing, People's Republic of China*

[b]*Department of Systems and Industrial Engineering, The University of Arizona, Tucson, AZ 85721, USA*

[c]*Department of Aerospace and Mechanical Engineering, The University of Arizona, Tucson, AZ 85721, USA*

[d]*Department of Mining and Geological Engineering, The University of Arizona, Tucson, AZ 85721, USA*

Received 22 February 1999; accepted 9 January 2000

Abstract

A mechatronic approach is studied here to design the mechanical system and controller concurrently for a robotic flexible manipulator. There is no coupling effects among these components which exit in traditional sequential design and this concurrent development leads to the global optimal performance. A linear quadratic regulator with output feedback is used to compare the results obtained from the traditional approach and this mechatronic approach. Using the mechatronic approach, optimal beam shapes as well as the associated optimal controllers for different feedback structures and for different objective functions can be achieved. Numerical results have indicated substantial improvements on performance. © 2000 Elsevier Science Ltd. All rights reserved.

Keywords: Manipulators; Optimal control; Design and construction; Dynamic modeling

* Corresponding author. Tel.: +1-520-621-6551; fax: +1-520-621-6555.
E-mail address: feiyue@sie.arizona.edu (F.-Y. Wang).

0957-4158/01/$ - see front matter
PII: S0957-4158(00)00004-0

1. Introduction

The link flexibility of a robotic manipulator must be considered in modeling and control when the manipulator is of large dimension or light weight. In the last decade, a significant effort has been made in modeling and control of one-link flexible manipulators [1,6–11]. However, one must realize that real-time control requires a dynamic model that must be computationally efficient. Therefore, accurate but complicated dynamic models are not proper for real-time control applications.

Control of a flexible manipulator is difficult since flexibility causes vibrations [2,4] and the so-called noncolocated control problem. It has been known that the problem of achieving stability is severe when noncolocated sensors and actuators are used for control. Another major problem in control design is robustness against model uncertainty and payload variations.

Two dual optimal design problems have been studied over the past few years [12–15]. Numerical results have indicated that a substantial increment in the fundamental frequency of vibration was obtained. But these studies were limited for open-loop flexible manipulators, that is, only designing the beam shape.

Most researchers design the mechanical construction, electronic driver and system controller for robotic flexible manipulators sequentially. This sequential design would lead to a local optimal performance, since coupling effects of mechanical, electronic, and control components of the manipulator system have not, simultaneously, been considered in the process. Therefore, the performance potential of a flexible manipulator could not be fully realized with the traditional design method.

The objective of this paper is to investigate the concurrent design of the mechanical system of a flexible manipulator with the controller at the beginning — the mechatronic approach. The basic idea is to design a better flexible manipulator such that its control problem would not be very critical for operational conditions. The overall system is global optimal for the controller as well as for the beam construction. Section 2 presents motion equations for flexible manipulators. Section 3 gives its finite approximation using the finite difference method. Section 4 presents the integrated system of link equation with DC motor dynamics, Section 5 describes the linear quadratic regulator design procedure, while Section 6 illustrates its mechatronic version by including link construction into the LQR design process. Several numerical examples are carried out in Section 7 to demonstrate the effectiveness of the proposed design method. Finally, Section 8 concludes the paper.

2. Dynamic equations of flexible manipulators

Consider a flexible manipulator carrying a tip load. It consists of a flexible beam of length L fixed on a rigid hub in the horizontal plane. The motion of the manipulator system is described by rigid rotation θ of the hub, flexible

displacement w and rotation ψ of the beam. The rotatory inertia is also considered. In the Euler–Bernoulli theory, $\psi = \partial w/\partial x = w'$. The total displacement v of the manipulator is defined as,

$$v(x, t) = w(x, t) + x\theta(t). \tag{1}$$

After a long process of simplification, the following dynamic equations are obtained in terms of the total displacement [7],

$$(Dv'')'' - \left(\rho S\ddot{v}'\right)' + \rho\ddot{v} = 0, \tag{2}$$

$$I_H\ddot{\theta} - Dv''(0) = \tau, \tag{3}$$

with boundary conditions,

$$x = 0, \quad v = 0, \quad v' = \theta; \tag{4}$$

$$x = L, \quad Dv'' + J_p\ddot{v}' + a_c M_p\ddot{v} = 0, \quad (Dv'')' - \rho S\ddot{v}' = M_p\left(\ddot{v} + a_c\ddot{v}'\right). \tag{5}$$

For the sake of numerical computation, the following dimensionless variables are introduced,

$$\xi = \frac{x}{L}, \quad t_{\text{new}} = \frac{t_{\text{old}}}{c}, \quad c^2 = \frac{M_0 L^3}{D_0}, \tag{6}$$

$$z(\xi) = \frac{v}{L}, \quad \alpha(\xi) = \frac{\rho(L\xi)L}{M_0}, \quad \beta(\xi) = \frac{D(L\xi)}{D_0}, \quad \delta(\xi) = \frac{S(L\xi)}{L^2} \tag{7}$$

$$\mu = \frac{M_p}{M_0}, \quad \eta = \frac{I_H}{M_0 L^2}, \quad \kappa = \frac{J_p}{M_0 L^2}, \quad \zeta = \frac{a_c}{L}. \tag{8}$$

where M_0 and D_0 are nominal values of beam mass and bending rigidity.

In terms of these new functions, variables, and parameters, the dynamic equations can be rewritten as follows,

$$\left(\beta z''\right)'' - (\alpha\delta\ddot{z}')' + \alpha\ddot{z} = 0, \tag{9}$$

$$\eta\ddot{\theta} - \beta(0)z(0)'' = \frac{\tau L}{D_0}; \tag{10}$$

with boundary conditions,

$$z(0) = 0, \quad z' = \theta; \tag{11}$$

$$\begin{aligned}&\beta(1)z''(1)+\kappa\ddot{z}'(1)+\zeta\mu\ddot{z}(1)=0,\\&\beta(z'')'(1)-\alpha\delta\ddot{z}'(1)=\mu\big[\ddot{z}(1)+\zeta\ddot{z}'(1)\big].\end{aligned}\tag{12}$$

A prime denotes the derivative with respect to coordinate ξ, and a dot represents the derivative with respect to time t_{new}.

3. Approximate state space equations

For the purpose of this study, we need a standard form of state space equations for a flexible manipulator system. The finite difference method (method of lines) is used to approximate partial differential equations described in the previous section with a set of ordinary differential equations. In this method, we substitute space derivatives by finite differences. The interval $(0<\xi<1)$ is divided into n uniform segments with $\Delta\xi=h=1/n$, and space derivatives are approximated by the finite difference. Define $\xi_i=ih$, and $z_i=z(ih,t)$, $\alpha_i=\alpha(ih)$, $\beta_i=\beta(ih)$, $\delta_i=\delta(ih)$, $i=0,1,\ldots,n$. Clearly, from the first two boundary conditions (11),

$$z_0=0,\quad z_{-1}=-\theta/n.\tag{13}$$

Therefore, Eq. (10) can be approximated by

$$\eta\ddot{\theta}+n\beta_0\theta-n^2\beta_0 z_1=\frac{\tau L}{D_0}\tag{14}$$

For $i=1$, we have,

$$\begin{aligned}&n^4\left[\beta_2 z_3-2(\beta_2+\beta_1)z_2+(\beta_2+4\beta_1+\beta_0)z_1-\beta_0\frac{\theta}{n}\right]\\&\quad+\big[\alpha_1+n^2(\alpha_1\delta_1+\alpha_0\delta_0)\big]\ddot{z}_1-n^2\alpha_1\delta_1\ddot{z}_2=0,\end{aligned}\tag{15}$$

for $i=2$, we have,

$$\begin{aligned}&n^4\Big[\beta_3 z_4-2(\beta_3+\beta_2)z_3+(\beta_3+4\beta_2+\beta_1)z_2-2(\beta_2+\beta_1)z_1\Big]\\&\quad+\big[\alpha_2+n^2(\alpha_3\delta_3+\alpha_2\delta_2)\big]\ddot{z}_2-n^2[\alpha_3\delta_3\ddot{z}_3+\alpha_2\delta_2\ddot{z}_1]=0,\end{aligned}\tag{16}$$

and for $i=3$ to $n-2$,

$$\begin{aligned}&n^4\Big[\beta_{i+1}z_{i+2}-2(\beta_{i+1}+\beta_i)z_{i+1}+(\beta_{i+1}+4\beta_i+\beta_{i-1})z_i\\&\quad-2(\beta_i+\beta_{i-1})z_{i-1}+\beta_{i-1}z_{i-2}\Big]+\big[\alpha_i+n^2(\alpha_{i+1}\delta_{i+1}+\alpha_i\delta_i)\big]\ddot{z}_i\\&\quad-n^2\big[\alpha_{i+1}\delta_{i+1}\ddot{z}_{i+1}+\alpha_i\delta_i\ddot{z}_{i-1}\big]=0.\end{aligned}\tag{17}$$

Since we have $n+1$ unknowns, $\boldsymbol{Z}=[\theta,z_1,\ldots,z_n]^{\mathrm{T}}$. We still need two more

equations. The difference equation for (9) at $i = n-1$ and the last boundary condition (12) can be written as,

$$n^2\left[\beta_n z_n'' - 2\beta_{n-1} z_{n-1}'' + \beta_{n-2} z_{n-2}''\right] + \left[\alpha_{n-1} + n^2(\alpha_{n-1}\delta_{n-1} + \alpha_{n-2}\delta_{n-2})\right]\ddot{z}_{n-1} - n^2[\alpha_{n-1}\delta_{n-1}\ddot{z}_n + \alpha_{n-2}\delta_{n-2}\ddot{z}_{n-2}] = 0,$$

$$\beta_n z_n'' + \kappa\ddot{z}_n + \zeta\mu\ddot{z}_n = 0, \tag{19}$$

$$n\beta_n z_n'' - n\beta_{n-1} z_{n-1}'' - n\alpha_n\delta_n(\ddot{z}_n - \ddot{z}_{n-1}) - \mu\left[\ddot{z}_n + n\zeta(\ddot{z}_n - \ddot{z}_{n-1})\right] = 0. \tag{20}$$

From Eq. (19) we have,

$$\beta_n z_n'' = -\kappa\ddot{z}_{n'} - \zeta\mu\ddot{z}_n.$$

Substituting this equation into Eqs. (18) and (20), we get the last two equations,

$$n^4\left[-2\beta_{n-1}z_n + (4\beta_{n-1} + \beta_{n-2})z_{n-1} - 2(\beta_{n-1} + 4\beta_{n-2})z_{n-2} + \beta_{n-2}z_{n-3}\right] - n^2\left[n\kappa + \zeta\mu + \alpha_{n-1}\delta_{n-1}\right]\ddot{z}_n + \left[\alpha_{n-1} + n^2(\alpha_{n-1}\delta_{n-1} + \alpha_{n-2}\delta_{n-2} + n\kappa)\right]\ddot{z}_{n-1} - n^2\alpha_{n-2}\delta_{n-2}\ddot{z}_{n-2} = 0, \tag{21}$$

$$n^3\beta_{n-1}(z_n - 2z_{n-1} + z_{n-2}) + (n^2\kappa + 2n\zeta\mu + n\alpha_n\delta_n + \mu)\ddot{z}_n - (n^2\kappa + n\alpha_n\delta_n + n\mu\zeta)\ddot{z}_{n-1} = 0. \tag{22}$$

Eqs. (14)–(17), (21), (22) can be written in a matrix form as,

$$M\cdot\ddot{Z} + K\cdot Z = \frac{\tau L}{D_0}B, \tag{23}$$

where

$$Z = [\theta, z_1, z_2, \ldots, z_{n-1}, z_n]^{\mathrm{T}}_{(n+1)}, \quad B = [1,0,0,\ldots,0,0]^{\mathrm{T}}_{n+1}$$

and M, K are mass and rigidity matrices obtained from the above equations.

Eq. (23) is the finite approximation of motion equations for flexible manipulators. Clearly, both M and K matrices are functions of beam construction, which provides us the basis for simultaneously optimal construction and control, based on the mechatronic formulation to be discussed later.

4. Overall system dynamic model

The actuator dynamics is incorporated with the link state-space equation into the overall system. A permanent magnet DC-motor is assumed to be the actuator for this study. Its dynamics is described by

$$J_m\ddot{\theta}_m + \left(B_m + \frac{K_b K_m}{R}\right)\dot{\theta}_m = \frac{K_m}{R}v_c - r\tau, \quad \theta = r\theta_m \tag{24}$$

where J_m is the actuator inertia, B_m the friction coefficient, K_m the torque constant, K_b the back emf constant, R the armature resistance, r the gear ratio, and θ_m, θ, v_c are the rotor rotation, hub rotation, and armature voltage, respectively. In general, all motor circuit parameters can be considered as design variables.

For sensor specification, we assume that the optical encoder geared on hub axis and the CCD camera clampped on hub will be used for hub rotation and tip deflection. The output vector here can be defined as,

$$y = \begin{bmatrix} \theta \\ w(1,t) \end{bmatrix} = \begin{bmatrix} \theta \\ z_n - \theta \end{bmatrix} \tag{25}$$

The state vector of a flexible manipulator is defined as,

$$q = \begin{bmatrix} q_1 \\ q_2 \end{bmatrix} = \begin{bmatrix} Z \\ \dot{Z} \end{bmatrix} \tag{26}$$

and the corresponding state-variable equations are,

$$\dot{q} = Aq + bu, \quad y = Cq, \quad u = \frac{J_m L}{r^2 R D_0}v_c \tag{27}$$

where

$$A = \begin{bmatrix} 0 & I \\ -\bar{M}^{-1}K & -k_1\bar{M}^{-1}Be_1 \end{bmatrix} \quad b = \begin{bmatrix} 0 \\ \bar{M}^{-1}B \end{bmatrix} \quad C = \begin{bmatrix} e_1 0 \\ e_2 0 \end{bmatrix} \tag{28}$$

and

$$\bar{M} = M + k_0 Be_1, \quad e_1 = [10\ldots0], \quad e_2 = [-10\ldots1], \quad k_0 = \frac{J_m L}{r^2 D_0}, \quad k_1 = \frac{L}{r^2 D_0}\left(B_m + \frac{K_b K_m}{R}\right) \tag{29}$$

Clearly, state equation (Eq. (27)) has incorporated manipulator motion (hub rotation and link deflection), actuator dynamics, as well as sensor specification. The system matrix A is a function of link construction (mass and stiffness distributions) and actuator design (motor parameters), while output matrix C is a function of beam position and tip deflection.

5. Linear quadratic regulator with output feedback

In this section we will give a brief description of the linear quadratic regulator

(LQR) with output feedback for flexible manipulators based on the approximate state model given by Eq. (27) in the previous section. This LQR formulation will be used as the basis for mechatronic design in the next section.

In LQR with output feedback, the controller has to be designed using output feedback instead of state feedback since states are generally not available for the control purpose. For the flexible manipulator system given by Eq. (27), the LQR controller will be a linear output feedback of the form

$$\mathrm{u} = -\mathfrak{R}\mathrm{y} \tag{30}$$

where $\mathfrak{R}$ is a matrix of constant feedback coefficients to be determined according to the following quadratic performance index (PI):

$$J(u) = \frac{1}{2}\int_{t_0}^{\infty}\left(q^{\mathrm{T}}(t)Qq(t) + u^{\mathrm{T}}(t)Ru(t)\right)\mathrm{d}t \tag{31}$$

where the Q, R are symmetric positive semidefinite weighting matrices.By substituting Eq. (30) into Eq. (27), the closed loop equations are

$$\dot{q} = (A - B\mathfrak{R}C)q = A_c q \tag{32}$$

Therefore, PI becomes

$$J = \frac{1}{2}\int_{t_0}^{\mathrm{T}} q^{\mathrm{T}}(t)\left(Q + C^{\mathrm{T}}\mathfrak{R}^{\mathrm{T}}R\mathfrak{R}C\right)q(t)\mathrm{d}t \tag{33}$$

Now, the LQR design problem is to choose gain $\mathfrak{R}$ such that J reaches its minimum value subject to the condition of stablizing the closed-loop system given by Eq. (34).Since $Q + C^{\mathrm{T}}\mathfrak{R}^{\mathrm{T}}R\mathfrak{R}C$ is a symmetric, positive-semidefinite matrix, under certain conditions [5], we will be able to find a symmetric, positive-semidefinite matrix P so that,

$$\frac{\mathrm{d}}{\mathrm{d}t}\left(q^{\mathrm{T}}Pq\right) = -q^{\mathrm{T}}\left(Q + C^{\mathrm{T}}\mathfrak{R}^{\mathrm{T}}R\mathfrak{R}C\right)q \tag{34}$$

Using P, then J can be rewritten as

$$J = \frac{1}{2}q^{\mathrm{T}}(0)Pq(0) - \frac{1}{2}\lim_{t\to\infty} q^{\mathrm{T}}(t)Pq(t) \tag{35}$$

Assuming that the system is asymptotically stable, the $q(t)$ vanishes with time, that is,

$$\lim_{t\to\infty} q^{\mathrm{T}}(t)Pq(t) = 0 \tag{36}$$

This leads to,

$$J = \frac{1}{2}q^{\mathrm{T}}(0)Pq(0) = \frac{1}{2}\mathrm{tr}(PX) \tag{37}$$

where the $n \times n$ symmetric matrix X is defined by $q(0)\mathrm{q}^{\mathrm{T}}(0)$, n is the dimension of q.

Furthermore, from Eqs. (32) and (34), we find that

$$A_c^{\mathrm{T}} P + P A_{\mathrm{c}} + C^{\mathrm{T}} \Re^{\mathrm{T}} R \Re C + Q = 0 \tag{38}$$

This is Lyapunov equation for solving P for given R and Q.Following the procedure described in [5], we arrive at the two additional equations for solving the LQR problem,

$$A_{\mathrm{c}} S + S A_{\mathrm{c}}^{\mathrm{T}} + X = 0 \tag{39}$$

$$\Re = R^{-1} B^{\mathrm{T}} P S C^{\mathrm{T}} (C S C^{\mathrm{T}})^{-1} \tag{40}$$

where S is a symmetric $n \times n$ matrix of Lagrange multipliers.

6. Concurrent design of construction and control

Traditionally, a mechanical engineer constructs the plant to be controlled first and then gives it to a control engineer, who then has to select an optimal control suitable to the given plant. Clearly, the plant will affect the optimal control and consequently, the optimal performance index. However, for our applications, the plant, i.e., the flexible beam, can be constructed differently. Therefore, one must evaluate different plant designs to improve the performance.

To make this clear, let us assume that Ω is the space of all feasible manipulator design and Λ is the feasible control space from motor output. Then our objective is to minimize the performance index with respect to link construction and control design, i.e.,

$$J^* = \inf_{(\mathrm{A},\ \mathrm{B},\ \mathrm{C}) \epsilon \Omega,\ \mathrm{u} \epsilon \Lambda} J(\mathrm{u};\mathrm{A},\ \mathrm{B},\ \mathrm{C}) \tag{41}$$

Obviously, this approach considers the mechanical, electronic, and control components of a robotic flexible manipulator as a whole and their developments are carried out simultaneously. Clearly, this concurrent design approach should lead to the global optimal performance because now the coupling effects of different parts of the manipulators are taken into account at the very beginning of the design process. This is the so-called mechatronic design approach.Since

$$J^* = \inf_{(\mathrm{A},\ \mathrm{B},\ \mathrm{C}) \epsilon \Omega,\ \ \mathrm{u} \epsilon \Lambda} J(\mathrm{u};\mathrm{A},\ \mathrm{B},\ \mathrm{C}) = \inf_{(\mathrm{A},\ \mathrm{B},\ \mathrm{C}) \epsilon \Omega} \left[\inf_{\mathrm{u} \epsilon \Lambda} J(\mathrm{u};\mathrm{A},\ \mathrm{B},\ \mathrm{C}) \right], \tag{42}$$

accordingly, the global optimization can be carried out in two steps. The first step (the inner-loop optimization) is to find the optimal control and its associated optimal value of the performance index based on a given plant (A, B, C), which is the traditional optimal control design problem. The second step (outer-loop

optimization) is to find the optimal feasible plant that will further minimize the performance index through the optimal controller. When the LQR formulation is used, this will lead to,

$$J^* = \inf_{(A,\,B,\,C)\in\Omega,\ u\in\Lambda} J(u;A,B,C) = \inf_{(A,\,B,\,C)\in\Omega}\left[\inf_{u\in\Lambda} J(u;A,B,C)\right]$$

$$= \inf_{(A,\,B,\,C)\in\Omega} \mathrm{tr}\left[P(A,B,C)X\right] \tag{43}$$

where P is found by solving the equations given in the previous section.

Based on our experience with the open-loop optimal design, the conventional optimization methods, such as gradient-based method, are not effective in solving the outer-loop optimization problem. Therefore, as for the open-loop design problems, here we will use the Improving Hit and Run (IHR) adaptive random search algorithm [3] for the outer-loop optimization. However, some modification must be made to IHR to ensure a constant volume during the optimization process since we assume that the total weight is a constraint.

For the sake of simplicity, we will only consider the situations where the area of cross-sections determines both the mass and stiffness distributions of the flexible beam (such as circular cross-sections or rectangular cross-sections with fixed width/height or fixed ratio of width and height). Our algorithm will be modified easily to other situations. Now the combined iterative procedure of the modified IHR and the LQR with output feedback can be specified as:

OLO — Outer-Loop Optimization

1. Set design vector $\Xi = [I_H,\ M_p,\ a_c,\ J_p,\ L,\ B,\ H,\ \gamma,\ \rho,\ E]$, and number of segments, N. Set step multiplier MUL to 1 and FACTOR to an appropriate constant. Set R, Q. Calculate X.
2. Calculate A_0 (uniform shape radius or width), set initial index = 0, call ILO to get the corresponding J.
3. Set minimum and maximum area constraints, $A_{\min}$ and $A_{\max}$ according to the beam strength requirement. Set $j = 1$.
4. Randomly select $N/2$ of the N segments and mark them with a 1 in vector $\boldsymbol{D}_j$ of length N. Mark the remaining $N/2$ segments with a -1. If N is odd, one randomly selected area will remain constant and will be marked by a 0.
5. Get $N/2$ samples from a $N(0,1)$ normal distribution and place them in each position of $\boldsymbol{D}_j$ where there is a 1. Place the negatives of this same sample in each position of $\boldsymbol{D}_j$ where there is a -1. This arrangement will ensure a constant volume during optimization. Here, $\boldsymbol{D}_j$ is called the direction vector.
6. Generate a step size, S, uniformly from $\boldsymbol{L}_j$, the set of feasible step sizes in the direction $\boldsymbol{D}_j$, where,

$$\boldsymbol{D}_j = \left\{S \in \Re : A_{\min} < A_j + SD_j < A_{\max}\right\}$$

   If $\boldsymbol{L}_j = \varnothing$, go to Step 4.
7. Set $S = S \times \mathrm{MUL}$, while $0 < \mathrm{MUL} \leq 1$.

8. Update the area vector, $\boldsymbol{A}_j$, set index = 1, call ILO to find J, if J is improved:

$$A_{j+1} = \left\{ \begin{array}{ll} A_j + SD_j & \text{if } J(A_j + SD_j) > J_j \\ A_j & \text{otherwise} \end{array} \right\}$$

   Set $J_{j+1} = J(A_{j+1})$.
9. If $J_{j+1} > J_j$, set TRIM $= \frac{|J_{j+1} - J_j|}{J_j} \times$ FACTOR and MUL = MUL − MUL × TRIM.
10. If the criteria is met, stop running. Otherwise, increase j and go to Step 4.
11. Stop: optimal feedback matrix $\Re^*$, and optimal performance index J^*; optimal flexible link structure A^*.

ILO — Inner-Loop Optimization

1. Initialization: $i = 0$, calculate β, δ, α based on A_j from OLO, construct A, B. Select an $\Re_0$ so that A_c is asymptotically stable
2. i-th iteration:
   Set $A_i = A - B\Re_i C$
   Solve the equations

$$A_i^{\mathrm{T}} P + P A_i + C^{\mathrm{T}} \Re_i^{\mathrm{T}} R \Re_i C + Q = 0, \quad A_i S + S A_i^{\mathrm{T}} + X = 0$$

   for P_i and S_i
   Set $J = \frac{1}{2}\mathrm{tr}(P_i X)$

3. Updation:
   Gain update direction: $\Delta\Re = \mathrm{R}^{-1} B^{\mathrm{T}} P_i S_i C^{\mathrm{T}} (\mathrm{C} S_i \mathrm{C}^{\mathrm{T}})^{-1} - \Re_i$
   Update gain: $\Re_{i+1} = \Re_i + \Gamma \Delta \Re$
   where α is chosen so that $A - \mathrm{B}\Re_{i+1}\mathrm{C}$ is asymptotically stable

4. Criteria:
   $J_{i+1} = \frac{1}{2}\mathrm{tr}(P_{i+1} X) \leq J_i$
   If $(J_{i+1} - J_i) \leq \epsilon$, the given criteria, go to step 5. Otherwise set $i = i + 1$ and go to step 2

5. Return to OLO
   Set $\Re = \Re_{i+1}$, $J = J_{i+1}$
   if index = 0, go to step 2; otherwise go to step 8.

Some numerical examples of using this algorithm will be given in the next section.

7. Numerical results

To verify the mechatronic method presented in Section 6, a rectangular aluminium flexible link with constant height is used for simulation. The beam weight keeps constant, this means the beam volume is constant. The mechatronic

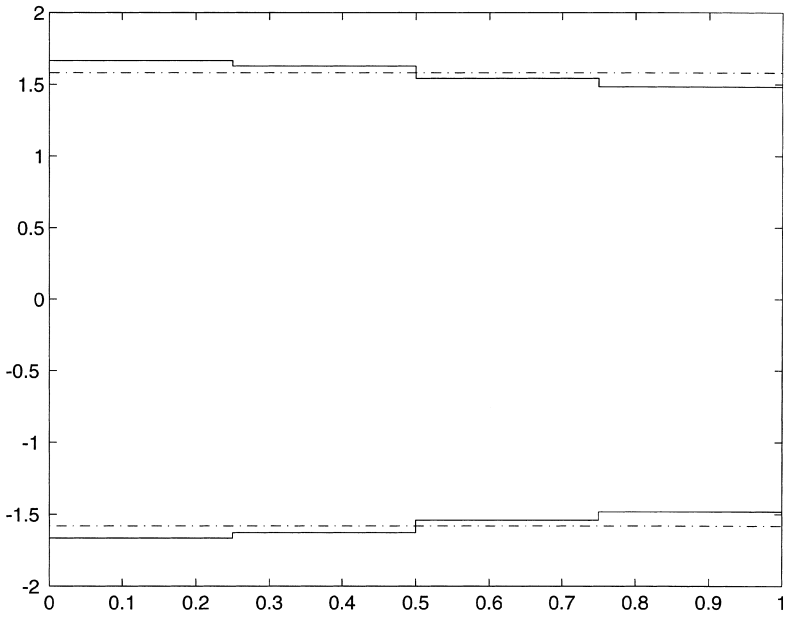

Fig. 1. Optimal shape for ($\{\theta\}$, 4, 100).

algorithm is to find the beam geometric shape, or the width distribution with the controller. This resultant shape is the optimal shape and the controller is optimal for the beam so that the performance index reaches the global minimum. The physical parameters of uniform beam which appear in the state dynamical model are given in Table 1.

From Eqs. (6)–(8)), we obtain the dimensionless constants which are used for the normalized link dynamics in Eqs. (9)–(12)). They are $\eta = 0.022$, $\kappa = 0.000214$, $\zeta = 0.035$, $c = 1.09$. The coefficients of DC motor in Eq. (24) are $R = 0.2$, $J_m = 0.2$, $B_m = 0.03$, $K_b = 0.1$, $K_m = 0.1$, $r = 1/47$. For the requirement of the beam strength, we set the maximum width $H_{\max} = 2 * H = 0.003175$ m, and

Table 1
Rectangular uniform beam physical parameters

M_0	Beam weight	0.5 kg	I_h	Hub inertia	0.0174 kgm^2
D_0	Nominal bending rigidity	0.44	γ	Beam density	2.713e + 3 kg/m^3
B	Beam width	1.587e −3 m	J_p	Tip inertia moment	1.5e−4 kgm^2
L	Beam length	1.098 m	M_p	Tip mass	0.2 kg
a_c	x-coordinate of tip mass	0.035 m	E	Young's modulus	6.63e + 9 kg/m^2
ρ	mass per unit length	0.4436 kg/m	H	beam height	0.103 m

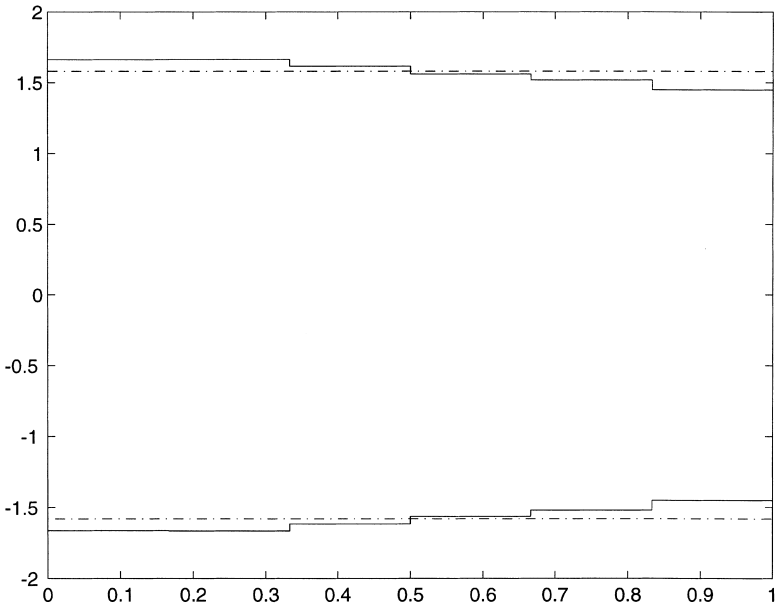

Fig. 2. Optimal shape for ($\{\theta\}$, 6, 100).

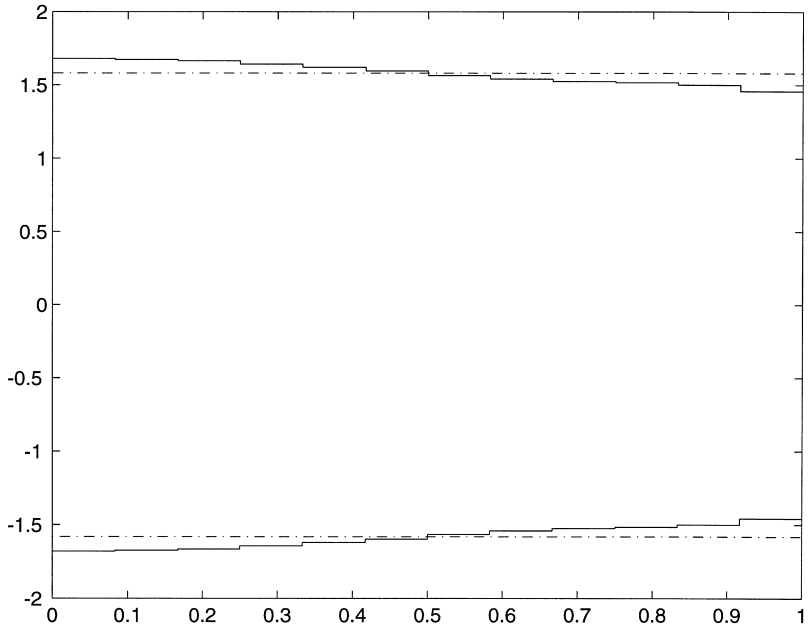

Fig. 3. Optimal shape for ($\{\theta\}$, 12, 100).

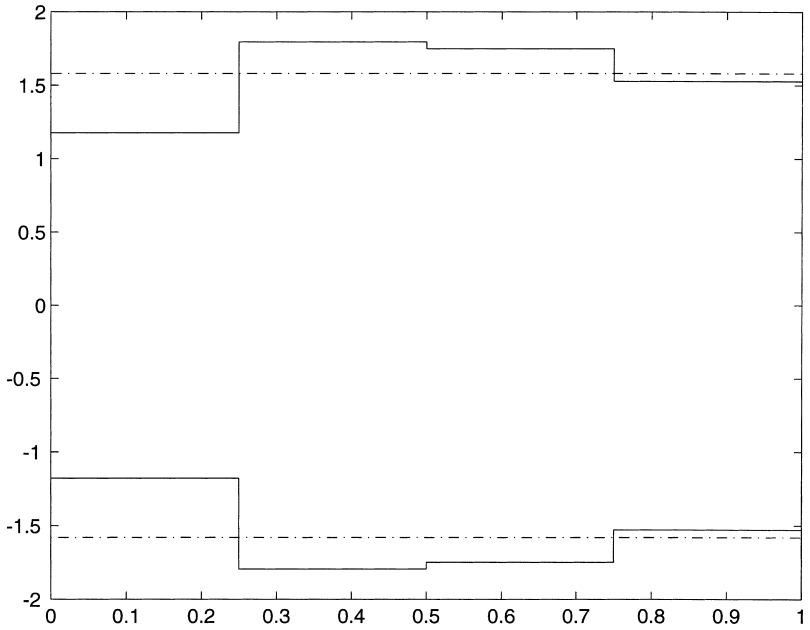

Fig. 4. Optimal shape for ($\{\theta, \omega\}$, 4, 100).

minimum width $H_{\min} = \frac{1}{4}H = 0.003965$ m. For the IHR algorithm, MUL = 1, FACTOR = 1, all other criteria are set to 0.000001.

The different output feedback strategies, combined with various number of segments n and state weighting matrix Q in Eq. (31) but $\mathrm{R} = \mathrm{I}$ are tested. The notation ({feedbacks}, number of segment, Q) is used here. Two feedbacks are considered, which are the hub angle θ feedback and the θ with the net tip displacement $w = z_n - \theta$. These feedbacks have very clear physical meanings and they are detectable as described in Section 4. The initial state is set to $q = [1,0,\ldots,0]^{\mathrm{T}}$. We set $\mathrm{Q} = 100 * I$, $n = 4, 6, 12$, with these two feedbacks. The best performance index are listed in Table 2, and the associated optimal controllers are

Table 2
Performance index ($\boldsymbol{Q} = 100 * \boldsymbol{I}$)

	$n = 4$	$n = 6$	$n = 12$
$\{\theta\}$ feedback — uniform shape	65704	65704	65704
$\{\theta\}$ feedback — optimal shape	45957	45964	45956
$\{\theta, z_n - \theta\}$ feedback — uniform shape	65424	65426	65423
$\{\theta, z_n - \theta\}$ feedback — optimal shape	45862	45865	45863

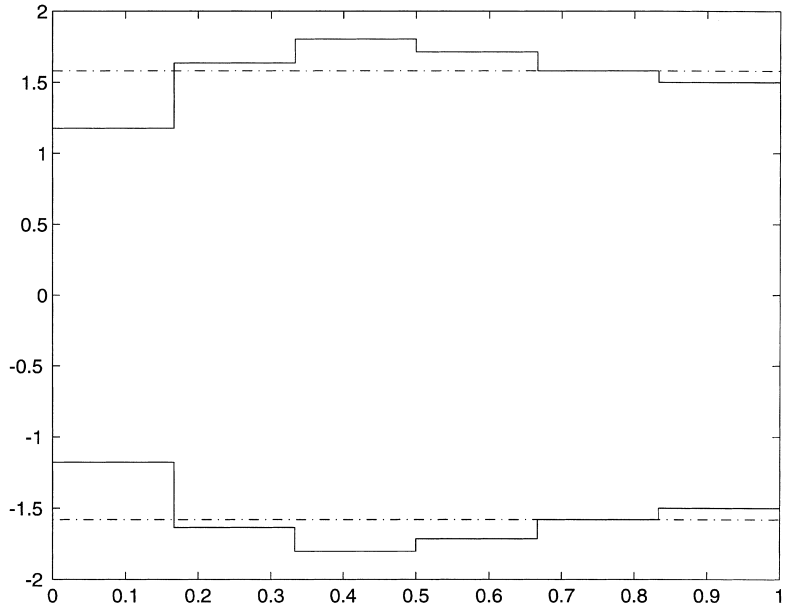

Fig. 5. Optimal shape for ($\{\theta, \omega\}$, 6, 100).

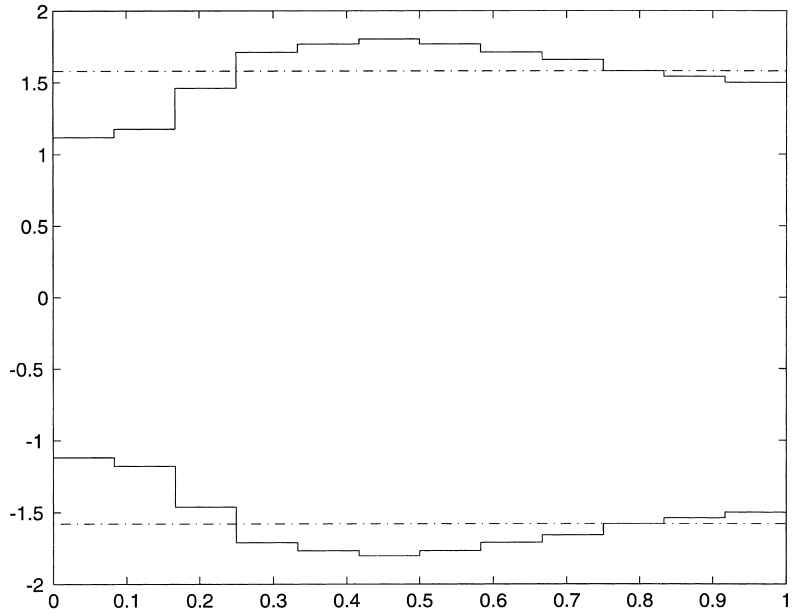

Fig. 6. Optimal shape for ($\{\theta, \omega\}$, 12, 100).

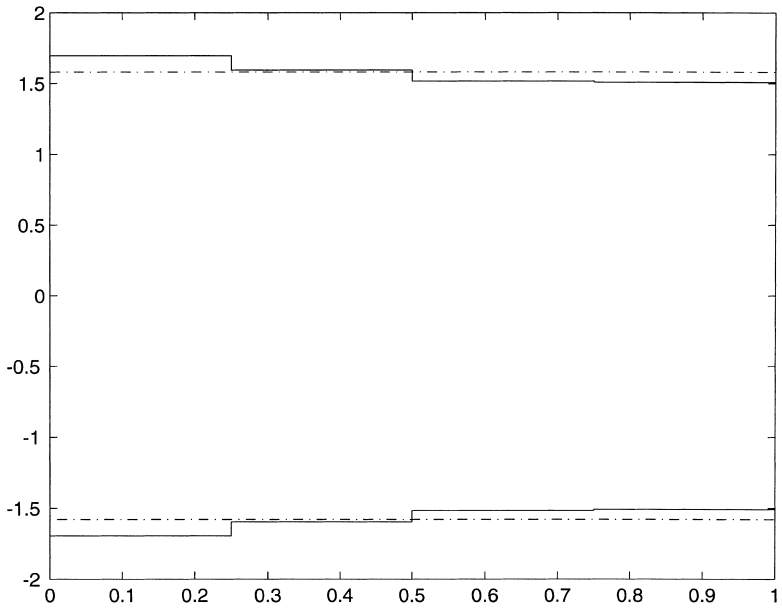

Fig. 7. Optimal shape for ({θ}, 4, 50).

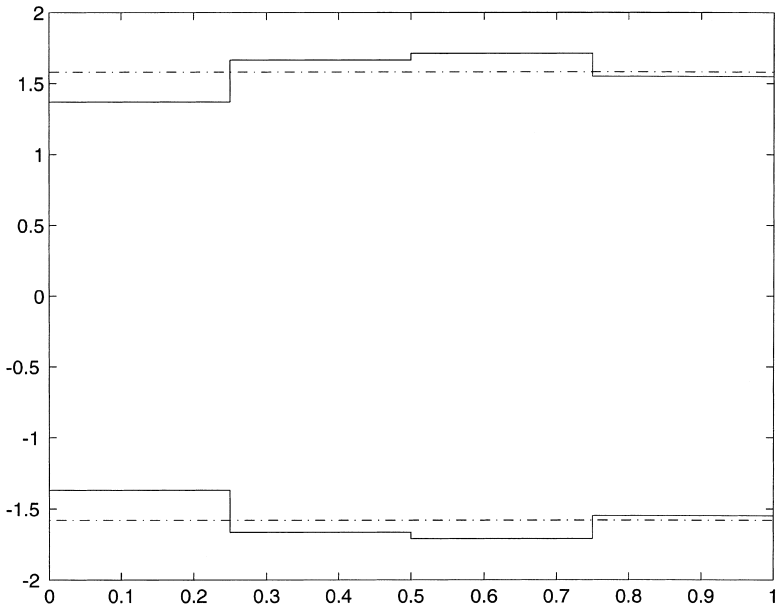

Fig. 8. Optimal shape for ({θ, ω}, 4, 50).

Table 3
Optimal feedback matrix ($Q = 100 * I$)

	$n = 4$	$n = 6$	$n = 12$
$\{\theta\}$ — uniform shape	3.674	3.674	3.674
$\{\theta\}$ — optimal shape	3.686	3.677	3.675
$\{\theta, z_n - \theta\}$ — uniform shape	(2.7599, −422.398)	(2.7599, −422.398)	(2.7599, −422.398)
$\{\theta, z_n - \theta\}$ — optimal shape	(2.498, −337.071)	(2.539, −380.396)	(2.423, −378.554)

listed in Table 3. The performance index for Q = 50, Q = 10 are illustrated in Table 4, and their controllers are in Table 5. Figs. 1–3 and 7 are the optimal shapes for $\{\theta\}$ feedback with different Q and segment number. But the shapes have one commom feature, that is, with a larger size at the hub end and smaller at the tip end. Figs. 4–6 and 8 are the optimal shapes for $\{\theta, w\}$ feedback. Their common feature is smaller dimensions at the ends. Step input responses of hub angle and tip deflection for $\{\theta, w\}$ feedback are as in Figs. 9 and 10. In all figures, the solid outline is for optimal shape or response, and the broken one is for those of uniform shape.

As shown in the above tables, the performance index is improved significantly, e.g., with $\{\theta\}$ feedback, $n = 4$, $Q = 100$, the performance index for uniform beam

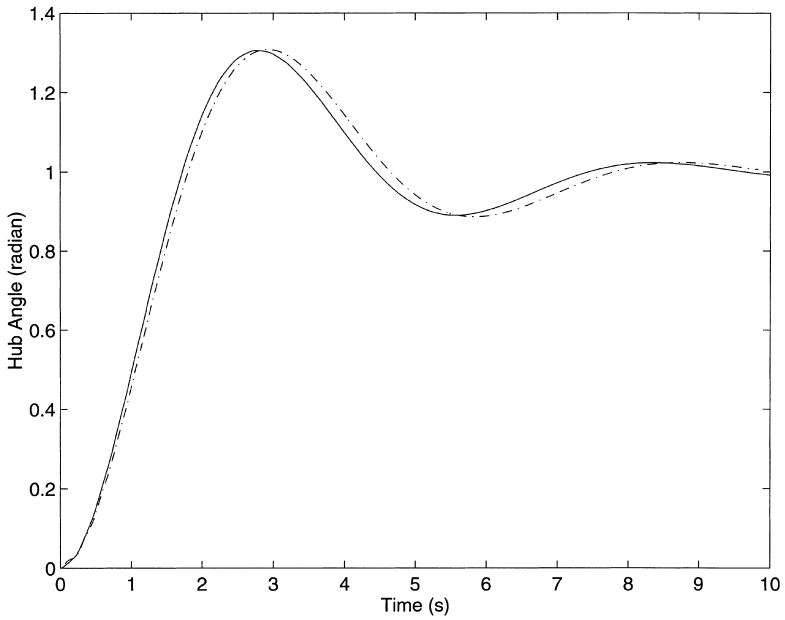

Fig. 9. Hub angle step input response for ($\{\theta, \omega\}$, 4, 100).

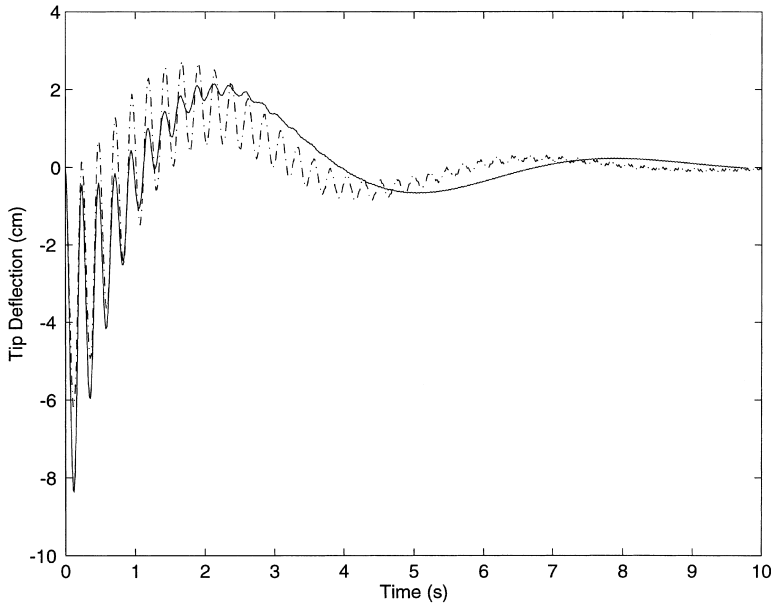

Fig. 10. Tip deflection step input response for ($\{\theta, \omega\}$, 4, 100).

is 65704 with its optimal controller $\Re = 3.674$. For its optimal shape, the performance index is 45957, which is decreased by 30% of that for the uniform beam, and the optimal controller is $\Re = 3.686$. It is also noticed that the performance index does not depend on the number of segments, because the final shape converges to its optimal shape. System with two variable feedbacks has lower performance index than those with one output variable feedback, since the former has more degrees of freedom to utilize. The improvement in performance is related to performance functions. For example, different Qs have different performance results. The step input of hub angle for the optimal shape has smaller rising time and tip deflection converges to stable much faster than for those of uniform shapes.

Table 4
Performance index with ($Q = 100 * I$, $50 * I$, $10 * I$)

	$\{\theta\}$	$\{\theta, z_n - \theta\}$
$Q = 50 * I$ — uniform shape	2611.373	2174.499
$Q = 50 * I$ — optimal shape	2540.470	2098.374
$Q = 10 * I$ — uniform shape	679.856	630.266
$Q = 10 * I$ — optimal shape	663.834	621.442

Table 5
Optimal feedback matrix with ($Q = 100 * I$, $50 * I$, $10 * I$)

	$\{\theta\}$	$\{\theta, z_n - \theta\}$
$Q = 50 * I$ — uniform shape	2.7599	(2.279, −395.458)
$Q = 50 * I$ — optimal shape	2.7303	(2.096, −335.370)
$Q = 10 * I$ — uniform shape	1.659	(1.604, −167.576)
$Q = 10 * I$ — optimal shape	1.653	(1.386, −166.142)

8. Conclusions

In this paper, the mechatronic design for both flexible beam linkage and controller are presented. The global optimized beam shape and controller parameters are obtained using an adaptive iterative algorithm with the accommodation of various geometrical constraints. Different output feedback strategies are investigated to evalute the impacts of various controller structures. The numerical results show that the flexible link can significantly improve upon the performance. The index can be chosen accordingly from system related functions depending on different applications, for instance, hub speed rising time, damping time, link tip deflection. Simulations for different optimizing variables, including motor parameters are further investigated. An experimental prototype is under construction for the verification of these simulation results. This method can be applied to other control system designs.

Acknowledgement

This work was supported in part by the Chinese National Natural Science Foundation and the University of Arizona Foundation.

References

[1] Cannon Jr. RH, Schmitz E. Precise control of flexible manipulators. In: Robotics Research: The First Intl. Symposium. Cambridge, MA: MIT Press, 1984. p. 841–61.
[2] Timoshenko S, Young DH, Weaver Jr. W. Vibration problems in engineering. 3rd ed. New York: Van Nostrand, 1957.
[3] Zabinsky ZB, Smith RL, McDonald JF, Romeigh HE, Kaufman DE. Improving hit-and-run for global optimization. Journal of global optimization 1993;3:171–92.
[4] Nguyen PK, Ravindran R, Carr R, Gossain DM, Doetsch KH. Structural flexibility of the shuttle remote manipulator system mechanical arm, SPAR Aero-Space Ltd., Tech. Info. AIAA, 1982.
[5] Lewis FL, Syrmos VL. Optimal control. New York: Wiley, 1995.
[6] Wang FY. Finding the maximum bandwidth of a flexible arm. In: Proc. of 32nd IEEE Conf. on Decision and Control, San Antonio, TX, USA, vol. 1. 1993. p. 619–25.
[7] Zhou PX, Williams MS, Wang FY. On closed-loop design of flexible robotic links. In: Proc. of IEEE International Conf. on Systems, Man, and Cybernetics, Beijing, China, Oct. 1996. p. 1712–7.

[8] Asada H, Park J-H, Rai S. A control-configured flexible arm: integrated structure/control design. In: IEEE Conf. on Robotics and Automation, Sacramento, CA, Vol. 3. 1991. p. 2356–62.
[9] Sakawa T, Matsuno F, Fukushima F. Modeling and feedback control of a flexible arm. Journal of Robotic Systems 1985;2:453–72.
[10] Yang GB, Donath M. Dynamic model of a one-link manipulator with both structural and joint flexibility. In: IEEE 1988 International Conference on Robotics and Automation, vol. 6, No. 3. 1988. p. 476–81.
[11] Wang F-Y. Optimum design of vibrating cantilevers: a classical problem revisited. J of Optimization Theory and Applications 1995;84(3):615–52.
[12] Wang FY. On the extremal fundamental frequencies of one-link flexible manipulators. Int J of Robotics Research 1994;13(2):162–72.
[13] Wang FY, Russell JL. Minimax optimum shape construction of flexible manipulators. In: Proc. of IEEE Int. Conf. on Decision and Control, Tucson, AZ. 1992. p. 311–6.
[14] Wang FY, Russell JL. Minimum-weight robot arm for a specified fundamental frequency. In: Proc. of IEEE Conference on Robotics and Automation, Atlanta, GA. 1993. p. 490–5.
[15] Wang FY. Optimum design of lightweight and flexible robot arms: a mechatronic approach. In: Proc. of the 1st Chinese World Congress on ICIA. 1993. p. 1160–5.